Geomorphology 308 (2018) 204–214

Contents lists available at ScienceDirect

Geomorphology

journal homepage: www.elsevier.com/locate/geomorph

Identifying the source of fluvial terrace deposits using XRF scanning and Canonical Discriminant Analysis: A case study of the Chihshang terraces, eastern Taiwan

Queenie Chang [a,b,c], Jian-Cheng Lee [b,*], Jyh-Jaan Hunag [a], Kuo-Yen Wei [a], Yue-Gau Chen [a], Timothy B. Byrne [c]

[a] Department of Geosciences, National Taiwan University, Taipei, Taiwan
[b] Institute of Earth Sciences, Academia Sinica, Taipei, Taiwan
[c] Center of Integrative Geosciences, University of Connecticut, Storrs, CT, USA

ARTICLE INFO

Article history:
Received 17 March 2016
Received in revised form 31 August 2017
Accepted 2 February 2018
Available online 07 February 2018

Keywords:
Fluvial terraces
Itrax-XRF scanning
Canonical Discriminant Analysis
Source identification

ABSTRACT

The source of fluvial deposits in terraces provides important information about the catchment fluvial processes and landform evolution. In this study, we propose a novel approach that combines high-resolution Itrax-XRF scanning and Canonical Discriminant Analysis (CDA) to identify the source of fine-grained fluvial terrace deposits. We apply this approach to a group of terraces that are located on the hanging wall of the Chihshang Fault in eastern Taiwan with two possible sources, the Coastal Range on the east and the Central Range on the west. Our results of standard samples from the two potential sources show distinct ranges of canonical variables, which provided a better separation ability than individual chemical elements. We then tested the possibility of using this approach by applying it to several samples with known sediment sources and obtain positive results. Applying this same approach to the fine-grained sediments in Chihshang terraces indicates that they are mostly composed of Coastal Range material but also contain some inputs from the Central Range. In two lowest terraces T1 and T2, the fine-grained deposits show significant Central Range component. For terrace T4, the results show less Central Range input and a trend of decreasing Central Range influences up section. The Coastal Range material becomes dominant in the two highest terraces T7 and T10. Sediments in terrace T5 appear to have been potentially altered by post-deposition chemical alteration processes and are not included in the analysis. Our results show that the change in source material in the terraces deposits was relatively gradual rather than the sharp changes suggested by the composition of the gravels and conglomerates. We suggest that this change in sources is related to the change in dominant fluvial processes that controlled by the tectonic activity.

1. Introduction

Understanding the source of fluvial sediments is important because it provides information about transport and erosion processes (Blair and McPherson, 1994; Ritter et al., 1995; Walling, 2013), and this information can be used to constrain past tectonic activity (Colombo et al., 2000; Mather, 2000; Marsaglia et al., 2010). Normally, the source or sources of fluvial sediments are identified by matching the lithology of the sediments with the composition of nearby outcrops or core samples that represent potential sources (Walling, 2013). For coarse-grained sediments, this can be accomplished by analyzing the color, texture, and composition of individual pebbles, cobbles and boulders and matching their composition with specific source areas. For the finer grained sediments, identifying the source is more challenging because the smaller grain size requires different and often more complicated and time-consuming approaches (e.g., Passmore and Macklin, 1994; Clapp et al., 2002; Walling, 2005; Douglas et al., 2006; Hughes et al., 2009). The purpose of this study is to provide an innovative approach to analyzing fine-grained sediments that combine automatic XRF-scanning with Canonical Discriminant Analysis (CDA) to efficiently identify the source of fine-grained fluvial terrace deposits.

In this study, we applied this approach to a group of Holocene fluvial terraces in the hanging wall of the Chihshang Fault in eastern Taiwan, characterized, in part, by conglomerate and pebble layers with different compositions, suggesting different sediment sources. Identifying the source of the terrace sediments will help constrain both the slip history of the Chihshang Fault as well as the evolution fluvial systems associated with the fault activities in eastern Taiwan.

2. Geological background

The Taiwan orogenic belt is a product of the Plio-Pleistocene convergence between the Eurasia and the Philippine Sea Plates (Ho, 1986;

* Corresponding author.
E-mail address: jclee@earth.sinica.edu.tw (J.-C. Lee).

https://doi.org/10.1016/j.geomorph.2018.02.011
0169-555X/

Teng, 1990). The collision between the Luzon volcanic arc and the Eurasia continental shelf resulted in the NE-SW-trending mountain belts. A 150-km-long, linear valley, the Longitudinal Valley, runs parallel to the mountain belt in eastern Taiwan and has long been recognized as the on-land plate suture because it separates rocks with different affinities; rocks to the west, i.e., the Central Range, were derived primarily from Eurasia whereas rocks to the east, i.e., the Coastal Range, were derived primarily from the Luzon arc (Fig. 1) (Hsu, 1962). The Central Range comprises exhumed Pre-Tertiary metamorphic complex and the overlying Tertiary slate belt, which are regarded as the continental basement (Yen et al., 1951; Yen, 1953; Chang, 1971, 1976; Jahn et al., 1986, 1990). The Coastal Range on the opposite side of the valley exposes arc volcanic rocks, fore-arc turbidite sequences, and a subduction olistostrome, the Lichi Melange (Teng and Wang, 1981; Teng and Lo, 1985; Teng et al., 1988). The Mio-Pliocene Lichi Mélange is particularly important for this study as it forms the bedrock underlying the terraces, and therefore one of the major sources of sediments in our study area. The Lichi Mélange is composed of sheared mudstone with different-sized exotic blocks, ranging in composition from deep-marine sandstones to large blocks pillowed lava and peridotite that together have been identified as a former ophiolite complex (Barrier and Muller, 1984; Page and Suppe, 1981).

The major active structure in the valley is the Longitudinal Valley Fault (LVF) – an east dipping thrust fault separates the Coastal Range from the Quaternary sediments that fill the valley. The 35-km-long Chihshang Fault, represents a segment of LVF and is located in south-central valley near the town of Chihshang. The Chihshang Fault is one of the most rapid creeping faults in the world with an average surface creeping rate of 2–3 cm yr^{-1} (Yu and Liu, 1989; Angelier et al., 1997, 2000; Lee et al., 2003; Mu et al., 2011). Even with continuous creeping slip, historical records show that the Chihshang Fault also generates earthquakes with Mw > 6.0 on a ~50-yrs reoccurrence interval (Lee et al., 2006; Shyu et al., 2007; Chen, 2009). Moreover, measurements for the past 30 years show that the creeping rate significantly decreased from ~2.5 cm yr^{-1} to ~1.5 cm yr^{-1} before the 2006 Chengkung earthquake (Mw = 6.8) and then returned to a normal, relatively steady creeping rate (Lee et al., 2003; Mu et al., 2011). Although recent fault activities are relatively well studied, the long-term slip patterns of the Chihshang Fault are still unclear. Therefore, the rate of uplift inferred from river terraces in the hanging wall of the fault has been the main target of tectonic geomorphological studies in this area.

River terraces developed on the hanging wall of the Chihshang Fault are mostly related to the incision of local tributaries sources on the Coastal Range. These terraces are mostly bedrock terraces distributed along the river valley and show thin layers of fluvial deposits composed of sediments from the local catchment. The Bieh River terraces developed along the west-flowing Bieh River represent one of the best studied examples of Holocene terraces (Gray, 2007). Here, ^{14}C dating of the terraces combined with the height of the terraces above the modern river suggest an average horizontal shorting rate associated with the Chihshang Fault is ~2 cm/yr for the last 1400 cal. yr B.P., which is similar to present-day activity rate (Angelier et al., 1997; Yu and Liu, 1989; Gray, 2007).

In addition to the relatively classic terraces with a clear relation to the modern river, another group of terraces appear to have a less clear relation to the modern river system. These terraces are also distributed on the hanging wall of the Chihshang thrust fault and form NNE-trending elongated shapes sub-parallel to the mapped trace of fault (Figs. 1c and 2). The terraces also occur where the west-verging Chihshang Fault cuts the toe of the alluvial fan associated with the east-flowing Xinwulyu River, suggesting a complicated formation processes. In one of the first relative detailed studies of this group of terraces, Chu (2007) dated four terraces that ranged in age from ca 300 yr BP to ca 6000 yr BP and attributed the formation of the terraces to tributaries coming from the Coastal Range. Liu et al. (2009) used the terrace ages from Chu (2007) and applied the nonlinear kinematic model to estimate the uplift history of the terraces. In contrast to Chu (2007), Liu et al. (2009) proposed that the terraces were related to uplift of the Xinwulyu River alluvial fan that originates from the Central Range, which lies west of both the Longitudinal Valley and the Chihshang fault.

In a more detailed study, Chang (2013) recognized ten levels of terraces characterized, in part, by conglomerates with compositions suggesting sources in both the Central and Coastal Ranges. Chang (2013) divided the terraces into ten levels based on the height of the terrace relative to the local alluvial fan surface. For example, T1 is composed of three segments that range in height from 17 to 19 m above the local fan whereas T10 is composed of two relatively small segments in the northern part of the study area and range in height from 78 to 90 m. These divisions, which are following here, are only based on the relative height of the terraces and are used primarily for descriptive purposes.

The terrace deposits are mainly conglomerates and show two compositions, suggesting two different source areas. The terraces were therefore divided into two units. A lower unit composed dominantly of metamorphic gravels such as vein quartz, meta-sandstone, marble, schist, and metabasite (Fig. 3a, b) and an upper unit represented mainly of gravels/sand intercalations composed of mostly un-metamorphosed sandstones and ultra-mafic rocks. The gravels of the lower unit appear to have been supplied by rivers and tributaries from the Central Range, probably the Xinwulyu River. In contrast, the gravels and sands of the upper unit are interpreted as debris/colluvium deposits (Fig. 3c) and fluvial channel deposits (Fig. 3d) from underlying Lichi Mélange.

The clear boundary between the upper and lower units observed in the field seems to suggest that the dominant source of the sediments shifted from the Central Range to the Coastal Range abruptly in each terrace as terrace formed. However, the source of the fine-grained deposits that interlayered with gravel deposits within the upper unit is unclear because the source of the fine-grained sediments is difficult to determine in the field (Fig. 3e). Whether the change in source was rapid or gradual is important for understanding the evolution of the river systems and local tectonics. As a result, the identifying of the source of the fine-grained deposits became the main target of this study.

Table 1
The information of the six trenches and corresponding terrace level in this study.

Trench	Location		Level of Terrace	Elevation (m)	Height difference[a] (m)	Total depth (m)
	X	Y				
1202FLa	121°14.88′ E	23°9.80′ N	T10	317	90	3.2
1210FNa	121°14.82′ E	23°9.10′ N	T7	301	56	4.8
1202FNa	121°14.71′ E	23°8.59′ N	T5	293	38	6.0
1202CYc	121°13.62′ E	23°6.59′ N	T4	296	32	4.6
1202FNb	121°14.26′ E	23°8.15′ N	T2	281	22	5.1
1202FNb	121°14.42′ E	23°8.47′ N	T1	275	17	3.3

[a] The height difference between the terrace surfaces and the footwall.

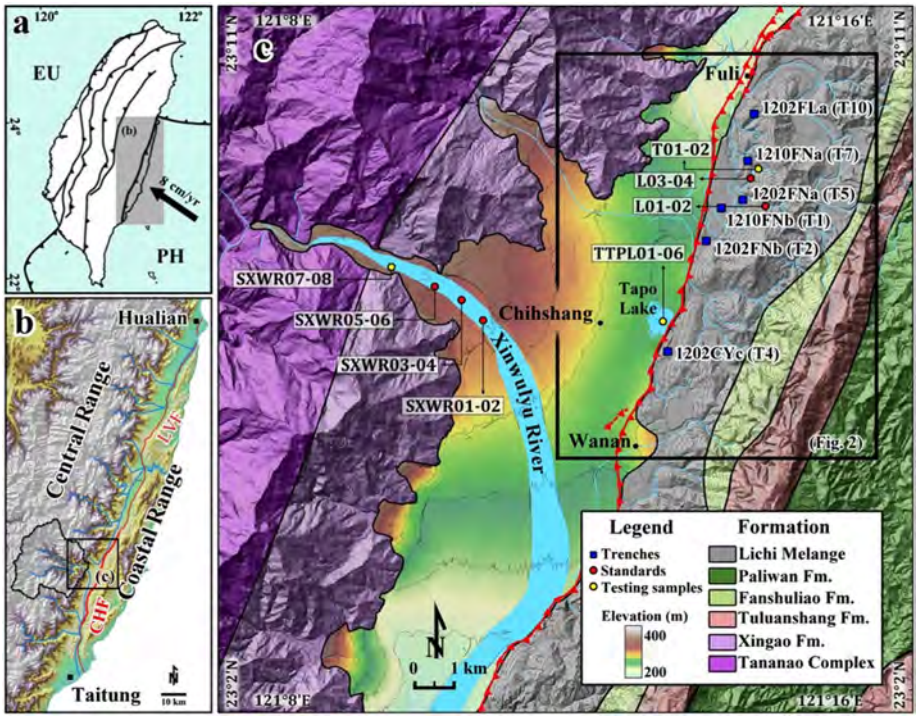

Fig. 1. Tectonic and geological setting of the study area. (a) Plate tectonic setting of Taiwan. The Philippine Sea plate (pH) is moving northwestward toward the Eurasian plate (EU) at the rate of ~8 cm/yr (Yu et al., 1997). (b) The Longitudinal Valley in eastern Taiwan and the location of the major active faults in red lines, the Longitudinal Valley Fault (LVF) and the Chihshang Fault (CHF). The river systems and the catchment of the Xinwulyu River are also shown in this figure. (c) Geology and topography map of the Chihshang area, showing the locations of trenches, standards, and testing samples in this study. The contour interval is 20 m. (For interpretation of the references to color in this figure legend, the reader is referred to the web version of this article.)

3. Methods

3.1. Sediment sampling

3.1.1. The side-coring technique for terrace sediments

Because of the heavy vegetation cover in this area, we excavated six 3–6 m-deep trenches on the surface of different levels of terraces for examining and sampling the fluvial terrace deposits. We developed the side-coring technique to sample the sediments from the sub vertical exposures that exposed by trenching. We oriented a meter-long, U-shaped plastic channel or trough vertically on the trench wall and pressed it into the fine-grained sediments. In some cases, a hammer was used to force as much sediments into the plastic channel as possible (Fig. 4b). A nylon fishing line was then run along the back side of the channel to release the sediment. The plastic channel was then gently pulled from the outcrop, retrieving as much sediment as possible. The "half-core" was then laid on the ground for measuring and photographing (Fig. 4c). Multiple plastic channels are needed depending on the length of the profile interested, so it is necessary to have overlap sampling between channels to avoid incomplete sampling at the edges.

3.1.2. Standard sediments

To characterize the source of the fine-grained terraces deposits, sediment samples taken directly from the source areas are required as standard sediments. Since the terrace deposits are mostly supplied by the rivers, the most suitable standard sediments are sediments from the present river bed, which represent the average material of the whole catchment. Therefore, six samples of river channel sediments from the Xinwulyu River (SXWR01–06) were collected as the standard sediments of the Central Range source. In the Coastal Range, modern river channels are lacking in sediments due to human construction. Since the sediments supplied to the Chihshang terraces only drain through the Lichi Mélange (Fig. 1c), mudstone samples from this formation are suitable for the Coastal Range source. Four mudstone samples from the bedrock of the Lichi Mélange (L01–04) were collected as the standard sediments.

3.1.3. Sediment samples for validity test

Four sets of samples with different scenarios of sediments deposition were prepared to test the validity and uncertainty of our approach by comparing them with the standard sediments (Fig. 1c). The Coastal Range-derived samples were collected from the fine-grained deposits of the terraces of the Alishan River (T01–02), a Coastal Range tributary without the interference of the Central Range rivers. Two subsets of the Xinwulyu River sand samples (SXWR07–08) were taken as the Central Range-derived deposits. Six samples were collected from the Tapo Pond deposits (TTPL01–06). The pond is located on the footwall to the west of the Chihshang Fault and is considered as a fault-related sag pond (Lee et al., 2006), where rivers from both the Coastal Range and the Central Range can reach it. Therefore, the deposits of this pond consist of sediments from both the ranges and represent a mixed-source situation. To further understand the characteristics of these deposits, we also prepared three samples (MIX01, MIX02, and MIX03), which are the artificial mixture of the two standards, with the ratios of the Coastal Range to the Central Range being 1:3, 1:1, and 3:1, respectively.

3.2. Itrax-XRF scanning

The conventional XRF technique requires time-consuming and destructive sample preparation processes, such as pressed pellets or fused beads. The Itrax-XRF core scanner (Itrax), which have facilitated the paleoenvironmental studies for the past decade (Croudace et al., 2006; Rothwell and Rack, 2006; Croudace et al., 2015; Rothwell and Croudace, 2015), is an automated instrument which can provide a semi-quantitative concentration of chemical elements in samples in a rapid, non-destructive manner. The scanning resolution can be high up to 0.1 mm. Here we use the Itrax to analyze the chemical signals of the fine-grained deposits in the upper unit of the Chihshang terraces.

The analysis was conducted at the Itrax-XRF Core Scanner Lab of National Taiwan University, using a Molybdenum (Mo) X-ray tube. The

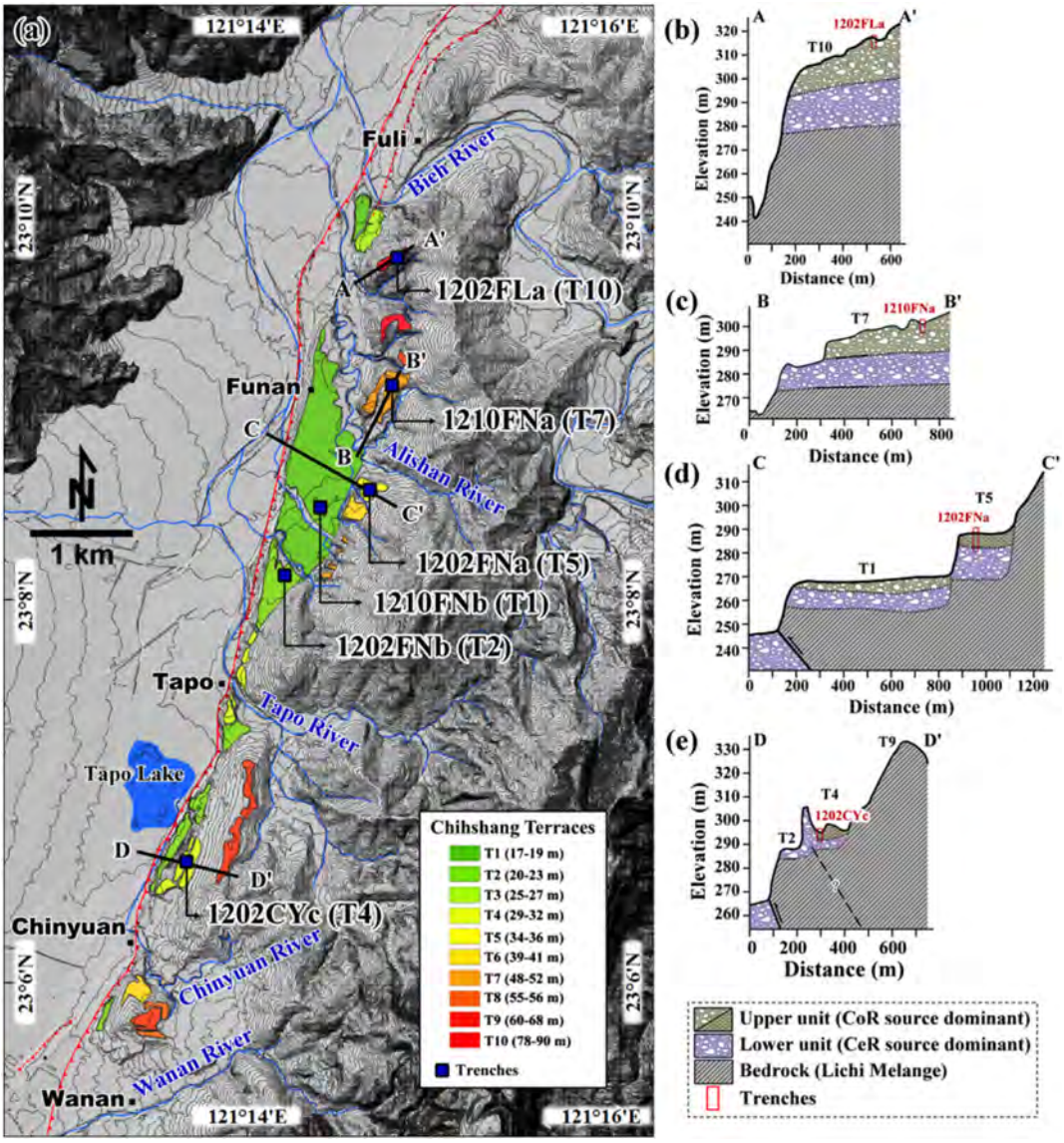

Fig. 2. (a) Distribution of the Chihshang terraces above the Longitudinal Valley at the mountain front of the Coastal Range. The terraces are divided into 10 levels based on the height difference between each terrace surface and the footwall of the Chihshang Fault. The contour interval is 5 m. (b)–(e) Schematic geological profiles of the terraces. The terrace deposits are typically composed of two units: lower unit and upper unit that composed predominantly material derived from the Central Range and the Coastal Range, respectively.

standard and testing sediments samples were first dried and ground into homogeneous powder. We adopted the sample preparation procedure of Huang et al. (2016) for the NTU Itrax-XRF scanning facility: a sample was filled into a 1-cm wide custom-made chlorine-free acrylic holders then compressed and covered by bi-directional PE film for protection and avoiding contamination. For the standard and testing sediments samples, we set the voltage of 30 kV, current of 25 mA, and exposure time of 15 s. Each sample was scanned discretely at 0.2 mm resolution, which is around 50 measured points for each sample. Except for the data near the edge of the sample holder, which was eliminated to avoid the edge effect, all the measurement records were used to calculate the average and standard deviation (shown in Tables S1 and S2 in Supplementary material). The half-cores samples from the six trenches, which did not require further sample preparation, were directly covered by the bi-directional PE film and scanned through the Itrax system at 1-mm resolution, with the voltage of 30 kV, the current of 32 mA, and exposure time of 15 s.

For estimating the relative abundances of major chemical elements, we used the software Q-spec 8.6.0 (Cox Analytical Systems) to calculate the peak area integrals of dispersive energy X-ray spectrum. Since the Itrax scanned the sediments without sample preprocessing, matrix effects such as mineral composition and grain size inhomogeneity or dilute effect caused by organic matter and pore water may influence the results of XRF measurements (Croudace et al., 2006; Tjallingii et al., 2007). To minimize this problem, it was suggested to use the ratios between elements for data analysis and interpretation (Croudace et al., 2006; Rothwell and Rack, 2006; Rothwell et al., 2006; Tjallingii et al., 2007; Löwemark et al., 2011). Conservative element such as Al, Ti and Rb are commonly used as the reference elements to normalize other elements (Rothwell and Rack, 2006; Rothwell et al., 2006; Löwemark et al., 2011; Hennekam and de Lange, 2012). In this study, we choose Ti as the reference elements, since the counts of Al and Rb are very low due to low detectability or concentration (Huang et al., 2016).

3.3. Canonical Discriminant Analysis (CDA)

Multivariate analysis has been widely applied to analyze various data on stratigraphy and sediments (Birks, 1987; Grant, 1990; Vasskog et al., 2012; Thomas et al., 2015). Here we applied Canonical

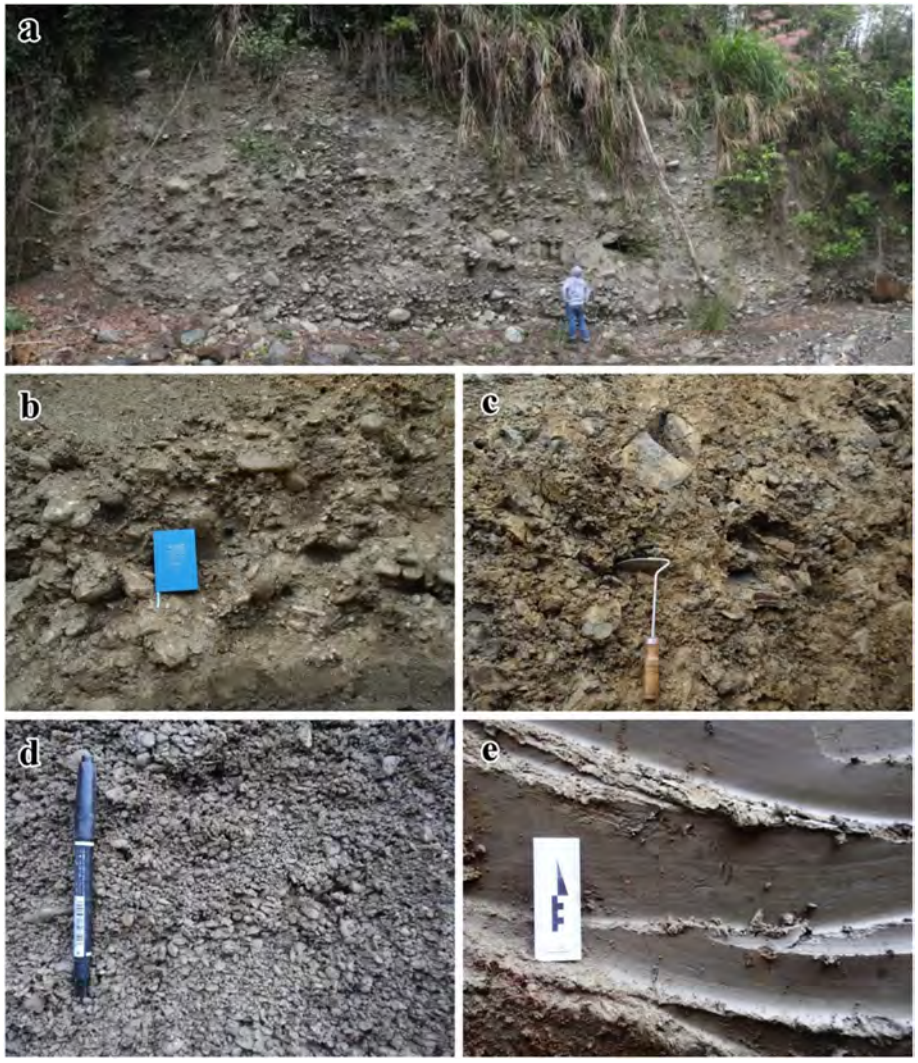

Fig. 3. Photograph of typical outcrops of sedimentary deposits of the Chihshang terraces. (a) and (b) Metamorphic rock gravel and sand of the lower unit derived from the Central Range (c) Angular sandstone gravels deposits of the upper unit, representing the debris deposits from local tributaries of the Coastal Range. (d) Well-sorted sandstone pebble deposits of the upper unit, indicating the channel deposits of tributaries from the Coastal Range. (e) Fine-grained deposits of the upper unit which represent standing water deposits such as lake or pond; the visible pattern on the outcrop is due to profile scratching and cleaning.

Discriminant Analysis (CDA) to deal with the great amount of data generated by XRF-scanning, and analyze the major differences in the chemical elements ratio to identify the sources of fine-grained sediments. CDA is often used to separate two or more groups with several variables by determining the canonical discriminant functions, which are the linear functions of all variables (Fisher, 1936; Rencher, 1992; Cruz-Castillo et al., 1994; Johnson and Wichern, 2007). The variables deduced from these functions are called canonical variables, which allow us to assess group membership of new observations (Roser and Korsch, 1988; Johnson and Wichern, 2007; Braun et al., 2013). Therefore, unlike other methods of multivariate analysis such as Principal Component Analysis (PCA) or Factor Analysis (FA), which investigate overall variation without concerning specific grouping (Bakraji et al., 2010; Vasskog et al., 2012), prior grouping criteria for classification are needed for CDA to generate the canonical discriminant function(s) (Rencher, 1992; Cruz-Castillo et al., 1994). In this study, the Central Range and the Coastal Range sources are the two prior grouping criteria.

The canonical loading, also known as the canonical structure or canonical correlation, represents correlations between observed variables and canonical variables, which allows us to examine the relative impact of each observed variable on CDA results. (Cruz-Castillo et al., 1994; Johnson and Wichern, 2007; SAS, 2009; Thomas et al., 2015).

We selected elements with high reproducibility assessed by the correlation coefficients ($R^2 > 0.80$) of the duplicate test results to perform CDA. The higher the correlation coefficients, the more reliable the Itrax-scanning results of these elements (Croudace et al., 2006; Jarvis et al., 2015; Rodríguez-Germade et al., 2015). Despite the reproducibility, elements that are rather low in correlation coefficients but exhibit significant differences between the sources were also considered. In this study, the correlation coefficients for Si, K, Ca, Ti, Mn, and Fe are all larger than 0.80. On the other hand, although the correlation coefficient of Sr is rather low ($R^2 = 0.46$), its ratio to Ti shows a distinctive difference between the two sources. Based on the aforementioned considerations, six element ratios respect to Ti (Fe/Ti, K/Ti, Mn/Ti, Si/Ti, Ca/Ti, and Sr/Ti) were applied for calculating the canonical variables in the analysis.

4. CDA results

4.1. CDA characteristics of the standard sediments samples

The CDA results for the standard sediments samples show the two sources can be efficiently separated by this method better than using just the element ratios (Fig. 5). The canonical variable results of the

Fig. 4. Photographs showing the typical trench profiles and sampling method. (a) Excavated trench reveals the upper and lower units (b) The side-coring technique is applied to obtain continuous terrace deposits samples. See text for detail description. (c) Example of terrace sediments samples. In this photo, it shows a ~2.5-m-long continuous profile sampled with three U-shaped plastic channels. There are arounds 10 cm overlaps between plastic channels.

Coastal Range have negative value, with the 2σ standard deviation fall between −7.0 and −3.8, while the Central Range are positive and between 0.5 and 4.9 with 2σ standard deviation.

As first mentioned by Fisher (1936), the purpose of CDA technique is to best separate two or more groups with multiple variables and to further classify new observations. The significant difference between groups is the key for successful classification. Our results of standard samples reveal that the Central Range and the Coastal Range sources have significant differences in chemical composition and can derive distinct ranges of the canonical variable for following analysis (Fig. 5).

The canonical loading values show that the CDA results of standard sediments agree with the geological characteristics of the source materials (Fig. 5h). The Central Range source is mainly composed of marble, schist, vein quartz, and metasandstone, thus is relatively rich in Si, Sr, and Ca (Yen et al., 1951; Yen, 1953; Stanley et al., 1981; Ho, 1986). This is reflected on the very high positive canonical loading of Si/Ti, Sr/Ti, and Ca/Ti, which means the abundance of Si, Sr, and Ca contributes to the positive canonical variables more significantly. On the other hand, The Coastal Range source contains more mafic materials, and are relatively abundant in Fe and K (Teng and Wang, 1981; Teng and Lo, 1985; Teng et al., 1988), which is reflected on the negative canonical loading of Fe/Ti and K/Ti.

4.2. CAD results of the sediment samples for validity test

To evaluate whether the canonical variable can properly indicate the sources, test classification was made using the samples with known sources. The samples include: (a) the Coastal Range (T01–02), (b) the Central Range (SXWR07–08), (c) mixed sources (TTPL01–06), and (d) lab-mixed sources (MIX01–03). The CDA classification results of testing sediments samples show that this method can correctly, to a large extent, identify the sources of sediments as predicted (Fig. 6).

The Coastal Range-derived samples from the Alishan River terrace deposits show the canonical variables between −5.8 and −8.6 (Fig. 6a), which is consistent with the 2σ range of the Coastal Range. The Central Range-derived samples from the Xinwulyu River sand have the canonical variables from 0.1 to 5.4, falling within the 2σ range of the Central Range (Fig. 6b). The canonical variables of the naturally-mixed samples are between −4.5 and −0.4, falling in the range of the Coastal Range and the Central Range (Fig. 6c). The lab-mixed samples have the canonical variables between −6.0 and −0.3

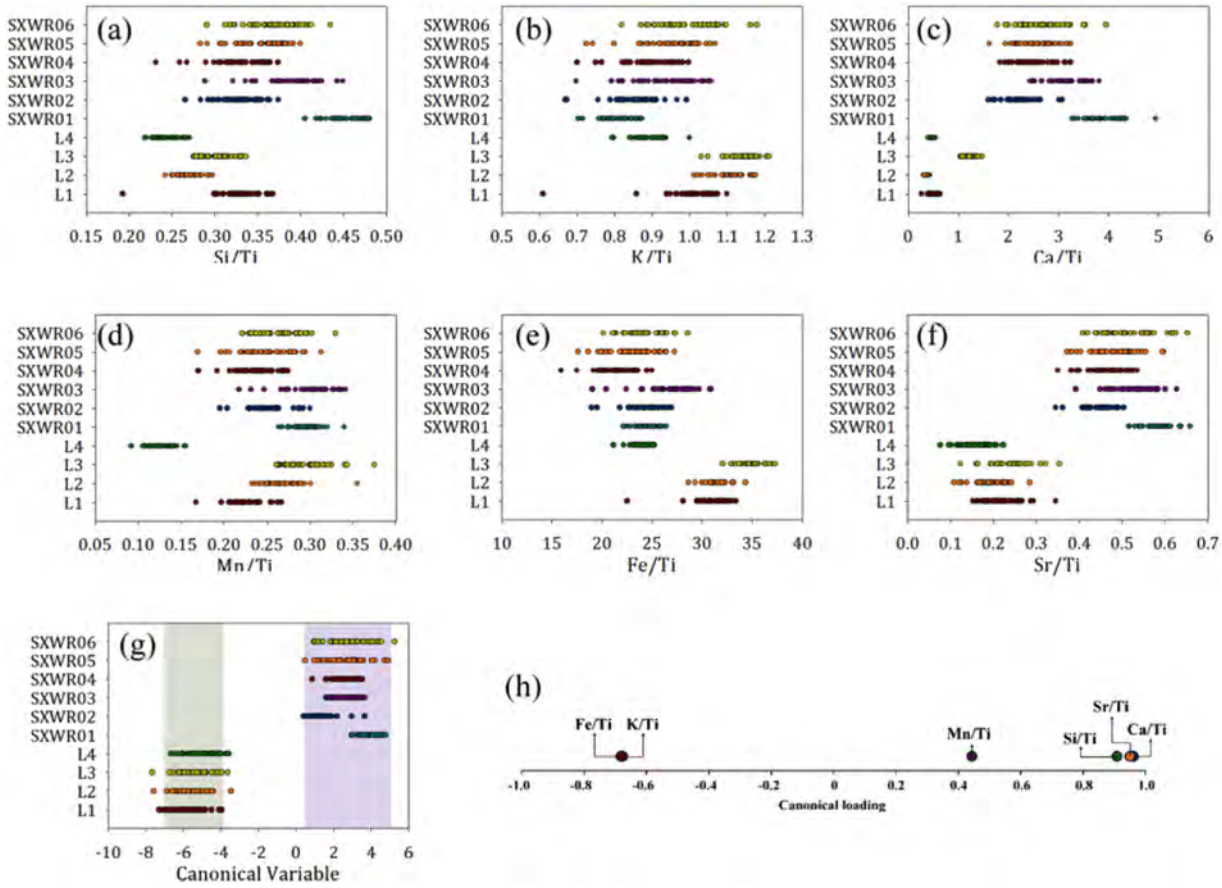

Fig. 5. Results of Itrax-XRF scanning and CDA of the standards from the Central Range (SXWR 01-06) and the Coastal Range (L01-04). (a)–(f) Individual element ratios of the standards. The points represent measurements on the different position of one sample (see text for detailed description). (g) Canonical variables of standards yield from the CDA. The green and purple shaded areas represent the 2σ range of the Coastal Range and the Central Range standards, respectively. (h) The canonical loading of six selected element ratios of the standards. (For interpretation of the references to color in this figure legend, the reader is referred to the web version of this article.)

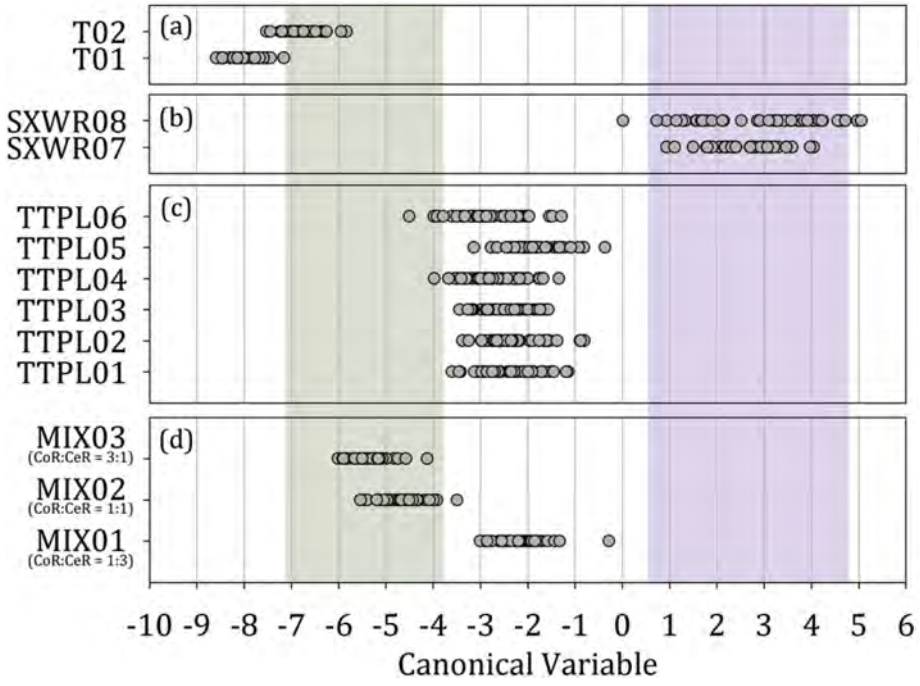

Fig. 6. The canonical variable of testing samples. (a) The Coastal Range-derived samples collected from the fine-grained deposits of the Alishan River terrace. (b) The Central Range-derived samples, which are subsets of the Xinwulyu River sand samples. (c) Naturally-mixed samples collected from the Tapo Pond deposits. (d) Lab-mixed samples. The green and purple shaded areas are same with Fig. 5g. (For interpretation of the references to color in this figure legend, the reader is referred to the web version of this article.)

(Fig. 6d). MIX01, which contains a higher percentage of the Central Range materials (CoR/CeR = 1/3), has the canonical variables between the two sources. The results of MIX02–03 lie in the range of the Coastal Range, which might suggest that mixed-source deposits with lower Central Range input percentage are less sensitive to be detected.

It is also noteworthy that the Itrax-XRF scanning derived the data sets in a semi-quantitative way, so the values and ranges of the element ratios from both sources are of uncertainties. This also highlights the benefits of using CDA to analyze the Itrax-XRF scanning results, since it analyzes the data structure and relationship among the variables, which is suitable for the semi-quantitative dataset (Fisher, 1936; Rencher, 1992; Cruz-Castillo et al., 1994; Johnson and Wichern, 2007).

4.3. Results of the terrace samples

The fine-grained sediments form two of the highest terraces, T10 and T7, yielded similar results, with most of their canonical variables falling within the range of the Coastal Range source, except for the lower layer in T10 which suggest some input from the Central Range. In T10, samples were collected from two fine-grained layers intercalated with gravel deposits (Fig. 7a). For the layer at 290–260 cm depth, the canonical variables lie around −4.0 and rapid increase to around 0.0 at the uppermost part, which suggesting mixing between two sources. For the layer at 120–70 cm depth and five fine-grained layers collected from T7 (Fig. 7b), the results mostly fall between −8.0 and −4.0, indicating that they are dominantly sourced from the Coastal Range.

The upper unit in terrace T5 is composed of 5-m thick massive mud deposition (Fig. 7c). Although the unit appear to be homogeneous deposits in the field, the CDA results are distributed over a wide range. At the beginning of the mud deposition around 450 cm depth, the canonical variable is extremely high and even exceeds the range of the Central Range source. Following a dramatic drop, the value then becomes negative and generally lies within the range of the Coastal Range at 450–400 cm depth. Above 400 cm depth, the results exhibit as fluctuations between two sources toward the upper part of the

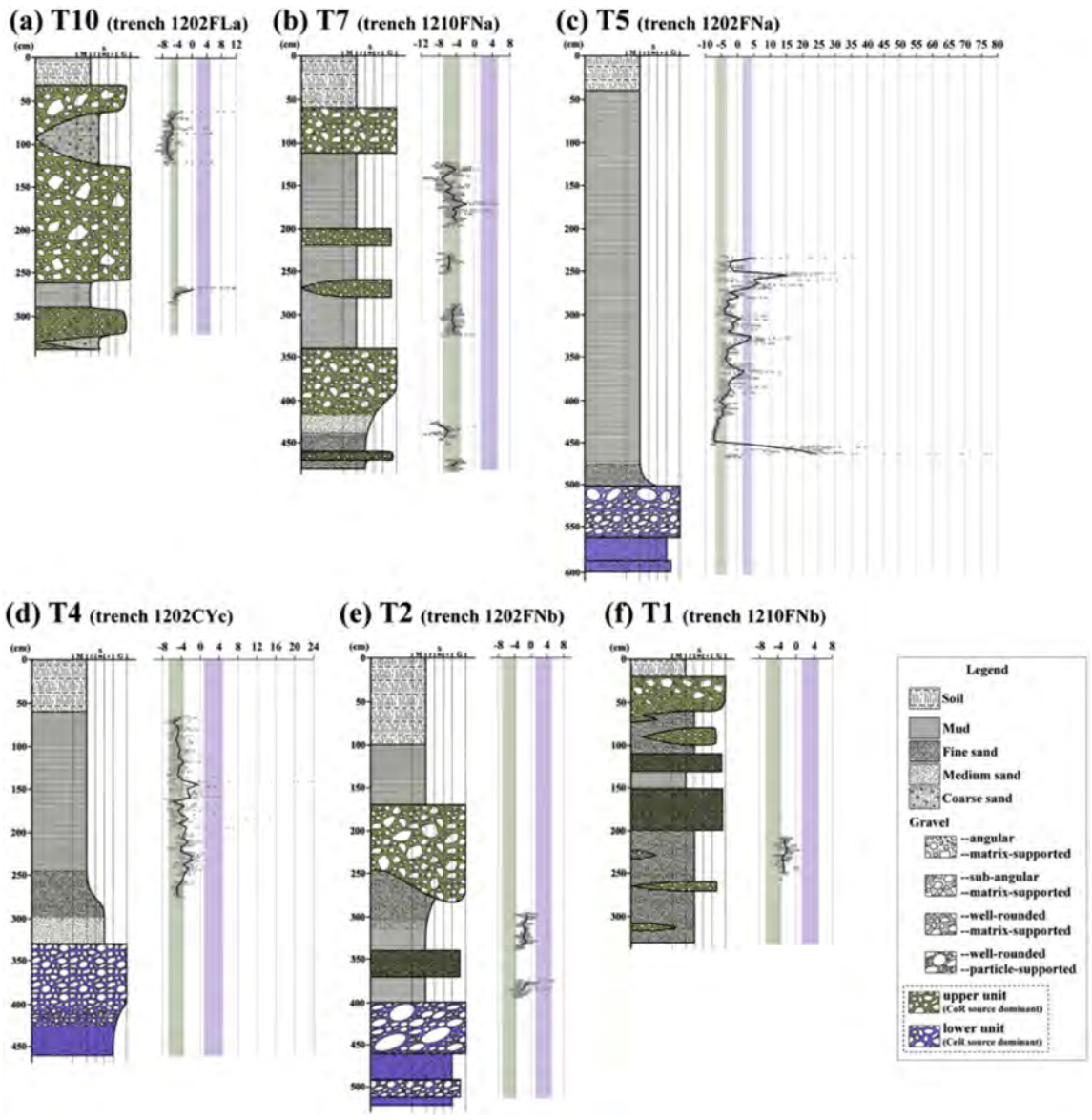

Fig. 7. The CDA results of the fine-grained sediments of the Chihshang terraces. The trench locations are shown in Fig. 1 and Fig. 2, and detail information is shown in Table 1. The points show canonical variables for every chemical analysis along the core (1-mm-resolution). The thick lines show the 50-mm-average of the same data. The green and purple shaded areas are the same as Fig. 5g. The geological columns are adopted after Chang (2013). (For interpretation of the references to color in this figure legend, the reader is referred to the web version of this article.)

deposits, with extremely high-value peaks at around 260–230 cm depth. These relatively anomalous values may reflect post-depositional redox processes, which will be discussed in the following section.

The upper unit in terrace T4 is composed of fine-grained deposits and no conglomerate composition (Fig. 7d). In this trench, samples were collected from 280 to 60 cm depth. From 280 to 150 cm, the canonical variables are more scattered between −6.0 and 0.0, which indicate mostly the Coastal Range source but are also largely mixed with the Central Range input. Above 150 cm depth, the results are more concentrated and fall with the range of the Coastal Range source, suggesting a decrease in the influences from the Central Range input through time.

Fine-grained deposits in two lowest terraces, T1 and T2, yielded similar CDA results. The samples were taken from one fine-grained layer in T1 and two in T2 (Fig. 7e and f). The canonical variables generally fall between −4.0 and 0.0, which is the range of mixed-sources that content high percentage of the Central Range input according to the results of testing samples (Fig. 6). Compared with the mixed-source material found in T4 (Fig. 7d), the fine-grained material in these two lower terraces are more significantly influenced by the Central Range material.

Summarizing the CDA results of all the six trenches, the Central Range input can be found in some of the fine-grained deposits with grater influences in lower terraces. T1 and T2 contain mixed-sources material with a large proportion of input from the Central Range. T4 also contains mixed-sources material, but the proportion of the Coastal Range input is larger, especially in the upper part of the terraces. As for higher terraces T7 and T10, the fine-grained deposits are predominantly coming from the Coastal Range.

4.4. Possible influences of Mn-oxyhydroxides

As described in the previous section, the trench in T5 shows abnormal high values that even exceeding the range of the Central Range source. To better understand the anomalous values, we examined the influences of the individual element profiles on canonical variables.

Of all six element ratios, the Mn/Ti value appears to be a major contribution to the variation of the canonical variable, especially regarding the high-value peaks in T5 (Fig. 8) That is, the higher the Mn content, the higher the canonical variable value. However, the overall Mn content in the metamorphic rock of the Central Range is rather low compared with the major elements such as Si or Ca (Yui et al., 1989, 1990). Therefore, the relative high Mn content in the terrace deposits is less likely caused by the input from the Central Range source. We hereafter propose an alternative interpretation: the Mn content in the fine-grained deposits on T5 is very likely contributed by post-depositional secondary minerals linked to changing redox conditions in standing water environment such as Mn-oxyhydroxides (Renaut and Gierlowski-Kordesch, 2010; Löwemark et al., 2012).

By contrast, at the bottom of the fine-grained deposits in T5 around 450–480 cm depth the high canonical variables seem to be related to not only high Mn/Ti value, but also high Ca/Ti and Sr/Ti. The latter two are dominantly derived from the Central Range source. As a result, the Central Range input may still be dominant in these bottom deposits.

As for the other terraces, the influences of Mn/Ti seem to be smaller. In T10 and T4, the results also show some extremely high positive-value peaks, but the running average suggests either the Coastal Range or the mixing sources. For T7, T2, and T1, the influences of Mn/Ti are relatively small. According to the discussion above, this implies minor post-depositional environment change, and therefore more reliable source identification results. That is, the Coastal Range material dominated on terrace T7 and mixing sources on terrace T2 and T1.

5. Implication on the tectonic and fluvial processes

As the Chihshang Fault is continuously thrusting, the terraces on the hanging wall were being uplifted away from the footwall and the Longitudinal Valley floor. Therefore, the dominant fluvial processes that formed the terraces transferred from lateral erosion and deposition of the Xinwulyu River to local deposition of the Coastal Range tributary rivers, and the influence of Xinwulyu River on the terrace surfaces fade away consequently (Chang, 2013). As a result, the metamorphic gravel deposits from the Central Range are primarily found in the lower part of the terraces.

On the other hand, our results of source identification indicate that the Central Range material can also be found in the fine-grained deposits in the upper section in the terraces. We argue that it is because the fine-grained sediments such as silt and clay can be transported farther than gravel. Therefore, at the early stage of terrace development when terrace surfaces were still close to the footwall, fine-grained sediments from the Central Range can reach the hanging wall through flooding of the Xinwulyu River. As the terraces being uplifted to heights that the flooding cannot reach, the Coastal Range would become the dominant source of sediments. The distribution of the fine-grained deposits that contain the Central Range material agrees with this argument. The influences of the Central Range input are stronger in lower terraces such as T1 and T2, where the fine-grained sediments are found closer to the Central Range conglomerate, while weaker in higher terraces such as T7 and T10.

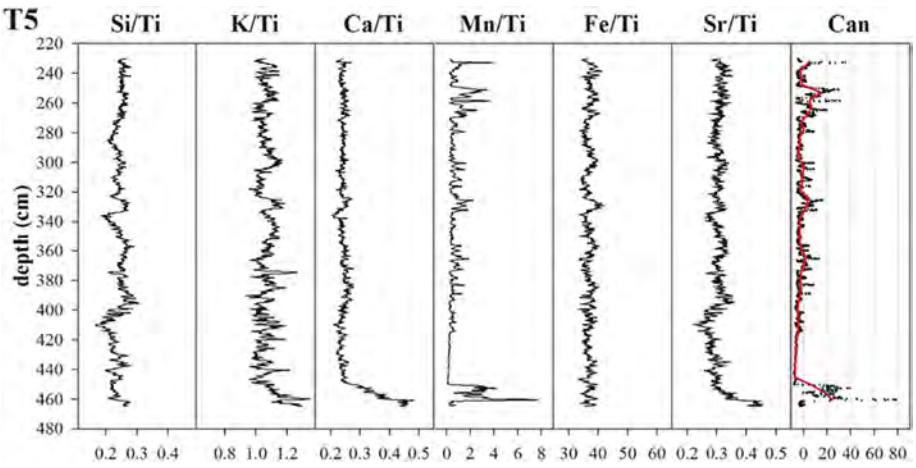

Fig. 8. 1-mm resolution element ratio profiles and canonical variable results of terrace T5. This figure shows that the intensity variation of the canonical variable is dominantly determined by Mn/Ti, while Ca/Ti and Sr/Ti might also contribute. The element ratio profiles of other terraces are shown in Supplementary material.

6. Conclusion

The high-resolution XRF-scanning technique combined with Canonical Discriminant Analysis (CDA) can efficiently identify the sediments coming from different sources with distinctive chemical composition in lithology. This is supported by our results of standards from the Coastal Range and the Central Range, which shows better separation than individual chemical element ratios. The results of testing samples also strengthened the validity of CDA to identify the sources of the fine-grained fluvial sediments.

The results of source identification of the fine-grained sediments in the Chihshang terraces reveal that the dominant source of the terrace deposits gradually transfers from the Central Range to the Coastal Range. This change in sediments source can extend to the fine-grained sediments that interlayered with the Coastal Range-sourced gravel deposits, instead of stopping at the boundary between conglomerate with different composition. The fine-grained deposits in lower terraces such as T1, T2, and T4 content more Central Range material than higher terraces like T7 and T10. We suggest that it is because the Chihshang terrace surfaces are continuously uplifted away from the Longitudinal Valley floor by the Chihshang fault, and therefore away from the influences of rivers derived from the Central Range. As a result, except for T5 that might be influenced by changing redox conditions such as Mn-oxyhydroxides, the source changes in Chihshang terraces deposits record the tectonic-related change in dominant fluvial processes that influenced the terraces forming.

Acknowledgements

We are grateful for many constructive comments and suggestions of the two anonymous Reviewers and the Editor Takashi Oguchi, which substantially improved this manuscript. This research was also supported by the Ministry of Science and Technology (MoST) of Taiwan (grants MOST 104-2116-M-001-020 and MOST 105-2116-M-001-001). This is a contribution of Institute of Earth Sciences, Academia Sinica, IESAS-2234.

Appendix A. Supplementary data

Supplementary data to this article can be found online at https://doi.org/10.1016/j.geomorph.2018.02.011.

References

Angelier, J., Chu, H.T., Lee, J.C., 1997. Shear concentration in a collision zone: kinematics of the Chihshang Fault as revealed by outcrop-scale quantification of active faulting, Longitudinal Valley, eastern Taiwan. Tectonophysics 274 (1–3), 117–143.

Angelier, J., Chu, H.T., Lee, J.C., Hu, J.C., 2000. Active faulting and earthquake hazard: the case study of the Chihshang Fault, Taiwan. J. Geodyn. 29 (3–5), 151–185.

Bakraji, E.H., Itlas, M., Abdulrahman, A., Issa, H., Abboud, R., 2010. X-ray fluorescence analysis for the study of fragments pottery excavated at Tell Jendares site, Syria, employing multivariate statistical analysis. J. Radioanal. Nucl. Ch. 285 (3), 455–460.

Barrier, E., Muller, C., 1984. New observations and discussion on the origin and age of the Lichi Mélange. Mem. Geol. Soc. China 6, 303–326.

Birks, H.J.B., 1987. Multivariate analysis of stratigraphic data in geology: a review. Chemom. Intell. Lab. Syst. 2 (1–3), 109–126.

Blair, T.C., McPherson, J., 1994. Alluvial fan processes and forms. In: Abrahams, A., Parsons, A. (Eds.), Geomorphology of Desert Environments. Springer, Netherlands, pp. 354–402.

Braun, M., Hubay, K., Magyari, E., Veres, D., Papp, I., Bálint, M., 2013. Using linear discriminant analysis (LDA) of bulk lake sediment geochemical data to reconstruct lateglacial climate changes in the South Carpathian Mountains. Quat. Int. 293, 114–122.

Chang, L.S., 1971. A biostratigraphic study of the so-called slate formation in Taiwan based on smaller Foraminifera: I. The EW cross-mountain highway. Proceedings of the Geological Society of China. 14, pp. 45–61.

Chang, L.S., 1976. The Lushanian stage in the central range of Taiwan and its fauna. In: Takaganagi, Y., Saito, T. (Eds.), Progress in Micropaleontology. Micropaleontology Press, New York, pp. 27–55.

Chang, Q., 2013. Evolution of the Holocene Uplifted Terraces Along the Chihshang Fault: Interactions Between Tectonics Uplift and Fluvial Sedimentation. (Master's thesis). National Taiwan University (in Chinese).

Chen, W.S., 2009. The fault slip long term velocity and recurrence period. Report of Central Geological Survey, pp. 31–40.

Chu, Y.K., 2007. Paleoseismology of the Chihshang Fault. (Master's thesis). National Taiwan University (in Chinese).

Clapp, E.M., Bierman, P.R., Caffee, M., 2002. Using 10Be and 26Al to determine sediment generation rates and identify sediment source areas in an arid region drainage basin. Geomorphology 45 (1–2), 89–104.

Colombo, F., Busquets, P., Ramos, E., Vergés, J., Ragona, D., 2000. Quaternary alluvial terraces in an active tectonic region: the San Juan River Valley, Andean Ranges, San Juan Province, Argentina. J. S. Am. Earth Sci. 13 (7), 611–626.

Croudace, I.W., Rindby, A., Rothwell, R.G., 2006. ITRAX: description and evaluation of a new multi-function X-ray core scanner. Special Republication-Geological Society of London. 267, pp. 51–63.

Croudace, I.W., Romano, E., Ausili, A., Bergamin, L., Rothwell, R.G., 2015. X-ray core scanners as an environmental forensics tool: a case study of polluted harbour sediment (Augusta Bay, Sicily). In: Croudace, I., Rothwell, R. (Eds.), Micro-XRF Studies of Sediment Cores: Applications of a Non-destructive Tool for the Environmental Sciences. Springer, Netherlands, Dordrecht, pp. 393–421.

Cruz-Castillo, J.G., Ganeshanandam, S., MacKay, B.R., Lawes, G.S., Lawoko, C.R.O., Woolley, D.J., 1994. Applications of canonical discriminant analysis in horticultural research. HortSci. 29 (10), 1115–1119.

Douglas, G.B., Ford, P.W., Palmer, M., Noble, R.M., Packett, R., 2006. Fitzroy River Basin, Queensland, Australia. I. Identification of sediment sources in impoundments and flood events. Environ. Chem. 3 (5), 364–376.

Fisher, R.A., 1936. The use of multiple measurements in taxonomic problems. Ann. Eugenics 7 (2), 179–188.

Grant, A., 1990. Multivariate statistical analyses of sediment geochemistry. Mar. Pollut. Bull. 21 (6), 297–299.

Gray, B.T., 2007. The Holocene Uplift of the Chihshang Segment of the Longitudinal Valley Fault at Fuli, Eastern Taiwan. (Master's thesis). Central Washington University.

Hennekam, R., de Lange, G., 2012. X-ray fluorescence core scanning of wet marine sediments: methods to improve quality and reproducibility of high-resolution paleoenvironmental records. Limnol. Oceanogr. Methods 10, 991–1003.

Ho, C.S., 1986. A synthesis of the geologic evolution of Taiwan. Tectonophysics 125 (1–3), 1–16.

Hsu, T.L., 1962. Recent faulting in the Longitudinal Valley of eastern Taiwan. Mem. Geol. Soc. China 1, 95–102.

Huang, J.J., Löwemark, L., Chang, Q., Lin, T.Y., Chen, H.F., Song, S.R., Wei, K.Y., 2016. Choosing optimal exposure times for XRF core-scanning: suggestions based on the analysis of geological reference materials. Geochem. Geophys. Geosyst. 17 (4), 1558–1566.

Hughes, A.O., Olley, J.M., Croke, J.C., McKergow, L.A., 2009. Sediment source changes over the last 250 years in a dry-tropical catchment, central Queensland, Australia. Geomorphology 104 (3–4), 262–275.

Jahn, B.M., Martineau, F., Peucat, J.J., Cornichet, J., 1986. Geochronology of the Tananao Schist complex, Taiwan, and its regional tectonic significance. Tectonophysics 125 (1–3), 103–124.

Jahn, B.M., Zhou, X.H., Li, J.L., 1990. Formation and tectonic evolution of southeastern China and Taiwan: isotopic and geochemical constraints. Tectonophysics 183 (1), 145–160.

Jarvis, S., Croudace, I.W., Rothwell, R.G., 2015. Parameter optimisation for the ITRAX core scanner. In: Croudace, I.W., Rothwell, R.G. (Eds.), Micro-XRF Studies of Sediment Cores: Applications of a Non-destructive Tool for the Environmental Sciences. Springer Netherlands, Dordrecht, pp. 535–562.

Johnson, R.A., Wichern, D.W., 2007. Applied Multivariate Statistical Analysis. Pearson Prentice Hall, Upper Saddle River, N.J.

Lee, J.C., Angelier, J., Chu, H.T., Hu, J.C., Jeng, F.S., Rau, R.J., 2003. Active fault creep variations at Chihshang, Taiwan, revealed by creep meter monitoring, 1998–2001. J. Geophys. Res. 108 (B11), 2528.

Lee, J.C., Chu, H.T., Angelier, J., Hu, J.C., Chen, H.Y., Yu, S.B., 2006. Quantitative analysis of surface coseismic faulting and postseismic creep accompanying the 2003, Mw = 6.5, Chengkung earthquake in eastern Taiwan. J. Geophys. Res. 111 (B2), B02405.

Liu, Y.C., Lee, J.C., Chen, R.F., 2009. The Holocene strath terraces of the Longitudinal Valley at Chihshang in eastern Taiwan and its implication to the activity of the Chihshang Fault. AGU Fall Meeting Abstract. 2009, pp. T33B–1893.

Löwemark, L., Chen, H.F., Yang, T.N., Kylander, M., Yu, E.F., Hsu, Y.W., Lee, T.Q., Song, S.R., Jarvis, S., 2011. Normalizing XRF-scanner data: a cautionary note on the interpretation of high-resolution records from organic-rich lakes. J. Asian Earth Sci. 40 (6), 1250–1256.

Löwemark, L., O'Regan, M., Hanebuth, T.J.J., Jakobsson, M., 2012. Late Quaternary spatial and temporal variability in Arctic deep-sea bioturbation and its relation to Mn cycles. Palaeogeogr. Palaeoclimatol. Palaeoecol. 365-366, 192–208.

Marsaglia, K.M., DeVaughn, A.M., James, D.E., Marden, M., 2010. Provenance of fluvial terrace sediments within the Waipaoa sedimentary system and their importance to New Zealand source-to-sink studies. Mar. Geol. 270 (1–4), 84–93.

Mather, A.E., 2000. Impact of headwater river capture on alluvial system development: an example from the Plio-Pleistocene of the Sorbas Basin, SE Spain. J. Geol. Soc. Lond. 157 (5), 957–966.

Mu, C.H., Angelier, J., Lee, J.C., Chu, H.T., Dong, J.J., 2011. Structure and Holocene evolution of an active creeping thrust fault: the Chihshang fault at Chinyuan (Taiwan). J. Struct. Geol. 33 (4), 743–755.

Page, B.M., Suppe, J., 1981. The Pliocene Lichi mélange of Taiwan: its plate-tectonic and olistostromal origin. Am. J. Sci. 281 (3), 193–227.

Passmore, D.G., Macklin, M.G., 1994. Provenance of fine-grained alluvium and late Holocene land-use change in the Tyne basin, northern England. Geomorphology 9 (2), 127–142.

Renaut, R.W., Gierlowski-Kordesch, E.H., 2010. Lakes. Facies Models 4, 541–575.

Rencher, A.C., 1992. Interpretation of canonical discriminant functions, canonical variates, and principal components. Am. Stat. 46 (3), 217–225.
Ritter, D.F., Kochel, R.C., Miller, J.R., 1995. Process Geomorphology. Wm. C, Brown Dubuque, IA.
Rodríguez-Germade, I., Rubio, B., Rey, D., Borrego, J., 2015. Detection and monitoring of REEs and related trace elements with an Itrax™ core scanner in the Ría de Huelva (SW Spain). Water Air Soil Pollut. 226 (5), 1–14.
Roser, B.P., Korsch, R.J., 1988. Provenance signatures of sandstone-mudstone suites determined using discriminant function analysis of major-element data. Chem. Geol. 67 (1–2), 119–139.
Rothwell, R.G., Croudace, I.W., 2015. Micro-XRF studies of sediment cores: a perspective on capability and application in the environmental sciences. In: Croudace, I.W., Rothwell, R.G. (Eds.), Micro-XRF Studies of Sediment Cores. Developments in Paleoenvironmental Research. Springer Netherlands, pp. 1–21.
Rothwell, R.G., Rack, F.R., 2006. New techniques in sediment core analysis: an introduction. Geol. Soc. Lond., Spec. Publ. 267 (1), 1–29.
Rothwell, R.G., Hoogakker, B., Thomson, J., Croudace, I.W., Frenz, M., 2006. Turbidite emplacement on the southern Balearic Abyssal Plain (western Mediterranean Sea) during marine isotope stages 1–3: an application of ITRAX XRF scanning of sediment cores to lithostratigraphic analysis. Geol. Soc. Lond., Spec. Publ. 267 (1), 79–98.
SAS Institute Inc, 2009. SAS Stat Studio 3.11: User's Guide. SAS Institute Inc., Cary, NC.
Shyu, J.B.H., Chung, L.H., Chen, Y.G., Lee, J.C., Sieh, K., 2007. Re-evaluation of the surface ruptures of the November 1951 earthquake series in eastern Taiwan, and its neotectonic implications. J. Asian Earth Sci. 31 (3), 317–331.
Stanley, R.S., Hill, L., Chang, H., Hu, H., 1981. A transect through the metamorphic core of the Central Mountains, southern Taiwan. Mem. Geol. Soc. China 4 (4), 443–473.
Teng, L.S., 1990. Geotectonic evolution of late Cenozoic arc-continent collision in Taiwan. Tectonophysics 183 (1–4), 57–76.
Teng, L.S., Lo, H.J., 1985. Sedimentary sequences in the island arc settings of the Coastal Range, eastern Taiwan. Acta Geol. Taiwan. 23, 77–98.
Teng, L.S., Wang, Y., 1981. Island arc system of the Coastal Range, eastern Taiwan. Proceedings of the Geological Society of China. 24, pp. 99–112.
Teng, L.S., Chen, W.S., Wang, Y., Song, S.R., Lo, H.J., 1988. Toward a comprehensive stratigraphic system of the Coastal Range, eastern Taiwan. Acta Geol. Taiwan. 26, 19–36.
Thomas, J., Joseph, S., Thrivikramji, K.P., 2015. Discriminant analysis for characterization of hydrochemistry of two mountain river basins of contrasting climates in the southern Western Ghats, India. Environ. Monit. Assess. 187 (6), 4589.
Tjallingii, R., Röhl, U., Kölling, M., Bickert, T., 2007. Influence of the water content on X-ray fluorescence core-scanning measurements in soft marine sediments. Geochem. Geophys. Geosyst. 8 (2), Q02004.
Vasskog, K., Paasche, Ø., Nesje, A., Boyle, J.F., Birks, H.J.B., 2012. A new approach for reconstructing glacier variability based on lake sediments recording input from more than one glacier. Quat. Res. 77 (1), 192–204.
Walling, D.E., 2005. Tracing suspended sediment sources in catchments and river systems. Sci. Total Environ. 344 (1–3), 159–184.
Walling, D.E., 2013. The evolution of sediment source fingerprinting investigations in fluvial systems. J. Soils Sediments 13 (10), 1658–1675.
Yen, T.P., 1953. On the occurrence of the late Paleozoic fossils in the metamorphic complex of Taiwan. Bull. Geol. Surv. Taiwan 4, 23–26.
Yen, T.P., Sheng, C.C., Keng, W.P., 1951. The discovery of fusuline limestone in the metamorphic complex of Taiwan. Bull. Geol. Surv. Taiwan 3, 23–25.
Yu, S.B., Liu, C.C., 1989. Fault creep on the central segment of the longitudinal valley fault, Eastern Taiwan. Proc. Geol. Soc. China 32 (3), 209–231.
Yu, S.B., Chen, H.Y., Kuo, L.C., 1997. Velocity field of GPS stations in the Taiwan area. Tectonophysics 274 (1-3), 41–59.
Yui, T.F., Lo, C.H., Wang Lee, C., 1989. Mineralogy and petrology of metamorphosed manganese-rich rocks at Santzanchi area, Eastern Taiwan. N. Jahrb. Miner. Abh 160, 249–268.
Yui, T.F., Wu, T.W., Jahn, B.M., 1990. Geochemistry and plate-tectonic significance of the metabasites from the Tananao Schist Complex of Taiwan. J. SE Asian Earth Sci. 4 (4), 357–368.